A TWO-PHASE BLIND RESTORATION ALGORITHM

C. M. Leung and W.-S. Lu

Department of Electrical and Computer Engineering
University of Victoria, Victoria, B.C., V8W 3P6

ABSTRACT

The aim of image restoration is to obtain a best possible estimate of an original image from a recorded version of the image. The effectiveness of restoration procedure requires the extent and the accuracy of the knowledge concerning the degradation process. If the degradation is unknown, it has to be estimated from the degraded image itself. In this paper, a new two-phase blind restoration algorithm is proposed. In the first phase of the algorithm, estimated power spectra of subimages of the original image is determined from the degraded image. In the second phase, a blind restoration algorithm is employed to obtain a restored image using estimated power spectra obtained in phase 1. Experimental results are presented to illustrate the proposed algorithm.

1. Introduction

Image restoration refers to the problem of removal or reduction of degradation in noisy blurred images. It consists mainly of three stages, namely, image formation modeling, blur function identification and application of certain restoration algorithms. For linear and spatially invariant blurring operators, the image formation model for digitized images can be described by [1]

$$g = Hf + n \tag{1}$$

where g and f represent the recorded and original images, respectively, H is the linear degradation, and n is the white noise. The success of an image restoration algorithm depends critically on the accuracy of the knowledge of the blurring operator H which is usually not known and has to be estimated from the observed degraded image g. It should be pointed out that the blurring operator H in (1) is usually an approximation of the original unknown image blur function which is difficult to express in an analytic form. Therefore a reasonable way of evaluating an identification process is to examine the quality of the image restored using the estimated $\hat{H}$. In this paper, we propose a new two-phase blind restoration algorithm, where an $\hat{H}$ is determined from the given degraded image g and a certain restoration algorithm (e.g., Tikhonov regularization) is used to obtain a restored image $\hat{f}$ in the second phase. In practice, the estimate $\hat{f}$ so obtained is usually a satisfactory version of f yet further improvement is possible. Experimental results indicate that in general the power spectra of $\hat{f}_m$ and f_m are approximately equal, i.e., $\mathcal{P}_{\hat{f}_m}(k,l) \approx \mathcal{P}_{f_m}(k,l)$ where $\hat{f}_m$ and f_m are corresponding subimages of $\hat{f}$ and f, respectively and $\mathcal{P}_q$ denotes the power spectrum of q. In phase 2 of the proposed algorithm, an improved estimate $\hat{\hat{f}}$ is obtained using a blind restoration algorithm [2] where $\hat{f}$ is taken to be the prototype image required by the algorithm. The purpose of using a prototype image is to provide an estimate of the power spectrum $\mathcal{P}_{f_m}(k,l)$. It was shown [2] that the power spectrum $|\mathcal{H}(k,l)|^2$ of the blurring operator H can be accurately estimated once $\mathcal{P}_{f_m}(k,l)$ is accurately estimated.

2. A Posteriori Blur Identification in Spectral Domain

The first step in restoring a degraded image is the determination of the type of degradation. If the degradation is unknown or if the analytical determination of the point spread function (PSF) of the degradation is too complex, one must estimate the degradation mechanism from the degraded image itself. There are many sources of degradation, including linear motion blur, defocusing blur, diffraction limit blur and charged coupled devices (CCD) interactions blur [2]. The blurs may be classified loosely into two groups by considering the geometrical shape of its PSFs — the group of 1-D linear motion PSFs and the group of circularly symmetric PSFs.

2.1 Linear Motion Blur

Linear motion blur is caused by relative motion between the object and the camera during exposure. The blurring is 1-D and its PSF is approximately given by [3]

$$h(k,l) = \begin{cases} \frac{1}{L+1} & 1 \le k \le L+1, \quad l = 1 \\ 0 & \text{otherwise} \end{cases} \tag{2}$$

where the blurring direction is assumed to be in the k-axis direction and L is an integer representing an approximate blurring distance. For linear motion type PSFs, it follows from (2) that it is only necessary to identify the direction of blurring and the blurring distance L. The frequency response of (2) is given by

$$\mathcal{H}(\omega_1,\omega_2) = \frac{1}{L+1} e^{j(-L\omega_1/2)} \frac{sin((L+1)\omega_1/2)}{sin(\omega_1/2)} \quad (3)$$

Assuming the given image g is of size $N \times N$, the discrete version of (3), i.e, the discrete Fourier Transform (DFT) of (2), is given by

$$\mathcal{H}(k,l) = \frac{1}{L+1} e^{jk(-L\pi/N)} \frac{sin(k((L+1)\pi/N))}{sin(k\pi/N)} \quad (4)$$

It follows from (3) that for given ω_2 the frequency response $\mathcal{H}(\omega_1,\omega_2)$ has zeros on the ω_1-axis with equal spacing of $2\pi/(L+1)$ and the first zero on the positive ω_1-axis is at $2\pi/(L+1)$. It is noted that $\mathcal{H}(k,l)$ in (4) has only approximate zero-values on the k-axis at points with approximately equal spacing of $[N/(L+1)]$ ($[x]$ denotes the largest integer in x) and its first approximate zero-value on the positive k-axis is at $[N/(L+1)]$. The approximate zero-values are exactly equal to zero only when $N/(L+1)$ is an integer. Hence approximate zero-value of $|\mathcal{H}(k,l)|$ (and so is $|\mathcal{H}(k,l)|^2$) occurs at interval of $[N/(L+1)]$ approximately. On the other hand, note that $\mathcal{P}_f(k,l)$ is usually of mound shape on some annular regions of the form

$$1 \le a \le \sqrt{(k-\frac{N}{2}+1)^2 + (l-\frac{N}{2}+1)^2} \le b \le N$$

and $\mathcal{P}_f(k,l)$ is significantly different from zero there. It is assumed in the rest of this paper that $a=1$ and $b=N$. Hence for every l, $\mathcal{P}_f(k,l)$ is monotonically decreasing and is significantly different from zero in $[N/2+1, N]$. In terms of power spectra, (1) gives

$$\mathcal{P}_g(k,l) = |\mathcal{H}(k,l)|^2 \mathcal{P}_g(k,l) + \mathcal{P}_n(k,l) \quad (5)$$

where it is assumed that the noise process is uncorrelated with f. In the absence of noise,

$$\mathcal{P}_g(k,l) = |\mathcal{H}(k,l)|^2 \mathcal{P}_f(k,l) \quad (6)$$

and hence the approximate zero-value pattern of $|\mathcal{H}(k,l)|^2$ must also be presented in $\mathcal{P}_g(k,l)$. The corresponding value $\mathcal{P}_g(k,l)$ of those approximate zero-values of $|\mathcal{H}(k,l)|$ may be amplified by $\mathcal{P}_f(k,l)$ and therefore it may no longer be small. Since $\mathcal{P}_f(k,l)$ is monotonically decreasing and $|\mathcal{H}(k,l)|^2$ is concave between any two consecutive 'zeros' on k-axis, it follows that a relative minimum of $\mathcal{P}_g(k,l)$ as well as $\log(\mathcal{P}_g(k,l))$ (because log is a monotonic function) occur near by the points $z_m = (N/2+1) + (mN)/(L+1), m = 1,\cdots,[(L+1)/2]$. Finally, we note that the most distinct and sharp pattern of minimum is exhibited in the section $\log(\mathcal{P}_g(k, N/2+1))$ which will be used in identifying parameter L.

The above discussion concludes that the linear motion type degradation can easily be identified by the image itself or by its power spectrum. It also indicates that once the degradation mechanism is classified as a linear motion blur its blurring direction as well as its sole parameter L can be readily obtained.

As an example, an 256×256 gray image 'Text' (Fig. 1(a)) is linearly blurred with $L=8$ and the blurred image is shown in Fig. 1(b). The plot $\log(\mathcal{P}_g(k,129))$ is shown in Fig. 1(d). It is seen that relative minimum occurs successively at $157th$, $185th$, $213rd$ and $241st$ pixel, i.e., at an interval of 28 pixels. Hence $256 = (157-129)(L+1)$ which gives $L=8$.

In the presence of noise with signal-noise-ratio (SNR) which is defined as

$$\text{SNR} = 10\log_{10}\frac{\text{variance of } Hf}{\text{variance of } n},$$

larger than 30 dB, it is possible to determine the PSF of the degradation in a way similarly to the above. Let the image g be divided into nonoverlapping subimages $\{g_m : m = 1,\cdots,M\}$ of equal size and let

$$\mathcal{P}_{g_s}(k,l) = \sum_{m=1}^{M} \mathcal{P}_{g_m}(k,l) \quad (7)$$

Then

$$\mathcal{P}_{g_s}(k,l) = |\mathcal{H}(k,l)|^2 \sum_{m=1}^{M} \mathcal{P}_{f_m}(k,l) + \sum_{m=1}^{M} \mathcal{P}_{n_m}(k,l) \quad (8)$$

where f_m and n_m are the corresponding subimages of f and n, respectively. As n is a white noise process, the term $\sum_{m=1}^{M} \mathcal{P}_{n_m}(k,l)$ would be nearly a constant. By the similar argument presented in the previous paragraph, for each l the graph of $\mathcal{P}_{g_s}(k,l)$ have relative minima occurring at approximately $z_m, m = 1,\cdots,[(L+1)/2]$ To demonstrate the proposed method, the linear blurred 'Text' in Fig. 1(b) is further contaminated by pseudo white Gaussian noise with SNR = 30 dB (Fig. 1(c)). The graph $\log(\mathcal{P}_{g_s}(k,33))$ is shown in Fig. 1(e) where subimage g_m is of size 64×64, $m = 1,\cdots,16$. Clearly relative minimum occurs consecutively at $40th$, $47th$, $56th$ and $62nd$ pixel, i.e., at an interval of approximately 7 pixels. Hence $L+1 \approx 64/7$ and $L=8$.

2.2 Defocusing Blur

The PSF of a defocusing blur is approximately constant within the circle of confusion (COC) and zero elsewhere [3]. This corresponds to the PSF in the spatial domain

$$h(x,y) = \begin{cases} 1/(\pi R) & x^2+y^2 \le R^2 \\ 0 & \text{otherwise} \end{cases} \tag{9}$$

where R is the radius of the COC. In the frequency domain, the corresponding PSF is given by

$$\mathcal{H}(\omega_1,\omega_2) = \frac{2J_1(R\rho)}{R\rho}, \quad \rho = \sqrt{\omega_1^2+\omega_2^2} \tag{10}$$

where $J_1(x)$ is the Bessel function of the first kind of first order. It is well known that $J_1(x)/x$ is a damping function with successive zeros with approximately equal spacing π. Note however that the first zero of $J_1(x)/x$ is at a distance 3.83 from the origin which is significantly different from π. Also $J_1(x)/x$ is equal to 0.5 when $x \to 0$. This shows that the zero pattern of $\mathcal{H}(\omega_1,\omega_2)$ as well as $\mathcal{P}_g(\omega_1,\omega_2)$ (in the absense of noise) in the frequency domain is a set of concentric circles with center at the origin spacing with a distance π/R and the radius of the innermost circle of zeros is $3.83/R$. It can be shown that the concentric circles intersect the interval $[0,\pi]$ on any axis at $(R-1)$ points. For example, when $R=5$, the concentric circles intersect the positive ω_1-axis at 0.77, 1.40, 2.03, 2.65, 3.28, $\cdots$, successively, and there are only 4 $(R-1)$ points in $[0,\pi]$.

Using an argument similar to that in Sec. 2.1, it is clear that in either noise-free or SNR $\geq$ 30dB case, the minimum value pattern of $|\mathcal{H}(k,l)|^2$ (or $\mathcal{P}_g(k,l)$) is the same as $|\mathcal{H}(\omega_1,\omega_2)|^2$ (or $\mathcal{P}_g(\omega_1,\omega_2)$). Hence the PSF can be claimed as a defocusing type when $\mathcal{P}_g(k,l)$ matches the above pattern. Once the PSF is identified as a defocusing blur, the parameter R can be estimated by plotting the graphs $\mathcal{P}_g(N/2+1,l)$ and/or $\mathcal{P}_g(k,N/2+1)$ and then counting the number r of its relative minima in the interval $[N/2+1,N]$. R is then equal to $r+1$. If subimages of size $N_s \times N_s$ are used, then R can be estimated by plotting the graph $\log(\mathcal{P}_{g_s}(N_s/2+1,l))$ (see (8)) and/or $\log(\mathcal{P}_{g_s}(k,N_s/2+1))$, and counting the number r of its relative minima in the interval $[N_s/2+1,N_s]$ and $R=r+1$ as required. To illustrate the above approach, a Lena (Fig. 2(a)) is defocused with radius of COC $R=5$ and SNR = 35 dB (Fig. 2(b)). The degraded Lena is then subdivided into 4 disjoint subimages of equal size 128×128. The graph $\log(\mathcal{P}_{g_s}(k,65))$ is shown in Fig. 2(c), from which 4 'periodic' relative minimum points are exhibited in the interval $[65,128]$. As a result, it is claimed that $R=5$.

2.3 Blur with Circularly Symmetric PSF

The PSFs of a large class of blurs with circularly symmetric shape can be roughly estimated using (9) with a certain degree of accuracy. Using the identification technique described in Sec. 2.2 and applying a conventional restoration algorithm, restored images $\hat{f}$ (see Sec. 1) are obtained and can be used as good prototype images in the blind restoration process.

3. A Blind Restoration Algorithm

For image system (1) in which the noise n is independent of the original image f, the power spectra of the system must satisfy (5), hence

$$\log|\mathcal{H}(k,l)|^2 = \log(\mathcal{P}_g(k,l)-\mathcal{P}_n(k,l)) - \log\mathcal{P}_f(k,l) \tag{11}$$

In order to obtain a good estimate of $\log|\mathcal{H}(k,l)|$, we generate a set of *block images* $\{g_m^b : m=1,\cdots,M\}$ from g. An $N\times N$ image g^b is called a *block image* of g with dimension N_b if it is of the form

$$g^b(k,l) = \begin{cases} g(k,l) & 1\le a\le k,\ l\le a+N_b-1\le N \\ 0 & \text{otherwise} \end{cases}$$

For each m, $(f_m^b,\ H,\ n_m^b,\ g_m^b)$ must satisfy (1) and hence (11). By taking average, we have

$$\log|\mathcal{H}| = \frac{1}{2M}\sum_{m=1}^{M}[\log(\mathcal{P}_{g_m^b}-\mathcal{P}_{n_m^b}) - \log\mathcal{P}_{f_m^b}] \tag{12}$$

Therefore, identification of $|\mathcal{H}(k,l)|$ requires power spectra estimation of $\mathcal{P}_{n_m^b}(k,l)$ and $\mathcal{P}_{f_m^b}(k,l)$. As noise n is white, estimation of $\mathcal{P}_{n_m^b}(k,l)$ can be obtained accurately in uniform zones of g. For estimation of $\mathcal{P}_{f_m^b}(k,l)$, it is suggested [4] that a *prototype image* of f is appropriate. By a *prototype image* of f, we mean an image similar to or has the same features as f. Conventionally, a sharp image with objects similar to those displayed on the degraded image is used as a prototype image in blind restoration. Here the estimate $\hat{f}$ obtained in phase 1 is used as a prototype image of f. This choice is more reasonable than the conventional one as at least $\mathcal{P}_{\hat{f}}(k,l) \approx \mathcal{P}_f(k,l)$.

Once $|\mathcal{H}(k,l)|$ is identified, a restored image is obtained by using the following modified Wiener filter [5]

$$W(k,l) = \frac{|\mathcal{H}(k,l)|}{|\mathcal{H}(k,l)|^2 + \frac{\alpha}{SNR}} \tag{13}$$

where α is a regularization parameter determined by trial and error.

Two experimental examples are used to illustrate the proposed algorithm. In the first example, the Lena

(Fig. 2(a)) was moved in the vertical direction by convolving with the following PSF

$$h(k,1) = \begin{cases} K & k = 1,\cdots,8 \\ Ke^{-k^2/100} & k = 9,\cdots,16 \\ 0 & \text{elsewhere} \end{cases} \tag{14}$$

where K is the value determined by the constraint

$$\sum_{k=1}^{16} h(k,1) = 1 \tag{15}$$

The blurred image was further contaminated by an additive white Gaussian noise with SNR = 35 dB. The resulting noisy and blurred image is shown in Fig. 3(a), and the restored image is shown in Fig. 3(b). In the second example, the Lena (Fig. 2(a)) was blurred by camera defocusing, and this can be obtained by convolving the original image with the PSF

$$h(k,l) = \begin{cases} Ke^{-(k^2+l^2)/300} & k,l = -5,\cdots,5 \\ 0 & \text{elsewhere} \end{cases} \tag{16}$$

and then adding a Gaussian noise with SNR = 35 dB, where K is the value determined by constraint (15). The resulting noisy image is shown in Fig. 4(a) and the restored image is shown in Fig. 4(b).

Acknowledgement

This work was supported by Micronet and IRIS.

References

[1] B. R. Hunt, "The application of constrained least squares estimation to image restoration by digital computer," *IEEE Trans. Computers*, vol. C-22, pp. 805-812, Sept. 1973.

[2] A. K. Jain, *Fundamentals of Digital Image Processing*, Englewood Cliffs, NJ: Prentice-Hall, 1989.

[3] R. L. Lagendijk and J. Biemond, *Iterative Identification and Restoration of Images*, Norwell, MA: Kluwer Academic Publishers, 1991.

[4] T. G. Stockham, Jr., T. M. Cannon and R. B. Ingebretsen, "Blind deconvolution through digital signal processing," *Proc. IEEE*, vol. 63, pp. 678-692, April 1975.

[5] C. M. Leung and W.-S. Lu, "A Variation of Wiener Filter in Image Restoration," in *Proc. IEEE Pacific Rim Conf. on Communications, Computers and Signal Processing*, Victoria, B. C., Canada, May 1993.

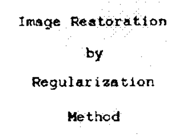

Fig. 1(a)

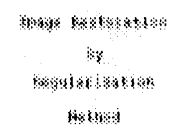

(b)

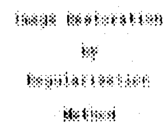

(c)

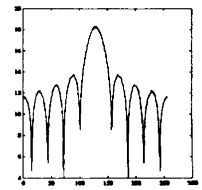

(d)

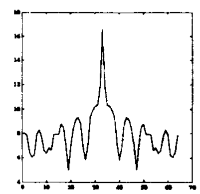

(e)

Fig. 2(a)

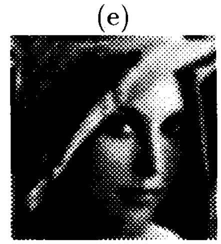

(b)

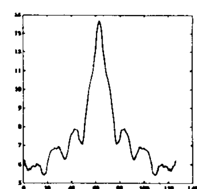

(c)

Fig. 3(a)

(b)

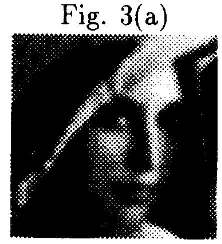

Fig. 4(a)

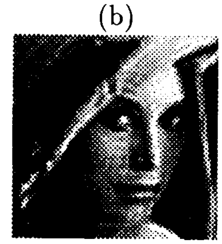

(b)